PHYSICAL REVIEW B **79**, 041308(R) (2009)

Renormalization factor and effective mass of the two-dimensional electron gas

Markus Holzmann,[1,2] Bernard Bernu,[1] Valerio Olevano,[3] Richard M. Martin,[4,5] and David M. Ceperley[5]
[1]*LPTMC, UMR 7600 of CNRS, Université Pierre et Marie Curie, 4 Place Jussieu, 75252 Paris, France*
[2]*LPMMC, CNRS-UJF, UMR 7644, CNRS, BP 166, 38042 Grenoble, France*
[3]*Institut Néel, CNRS-UJF, 38042 Grenoble, France*
[4]*Department of Applied Physics, Stanford University, Stanford, California 94305, USA*
[5]*Department of Physics, University of Illinois, 1110 W. Green Street, Urbana, Illinois 61801, USA*
(Received 16 December 2008; published 30 January 2009)

We calculate the momentum distribution of the Fermi-liquid phase of the homogeneous two-dimensional electron gas. We show that close to the Fermi surface, the momentum distribution of a finite system with N electrons approaches its thermodynamic limit slowly, with leading-order corrections scaling as $N^{-1/4}$. These corrections dominate the extrapolation of the renormalization factor Z and the single-particle effective mass m^* to the infinite system size. We show how convergence can be improved using analytical corrections. In the range $1 \le r_s \le 10$, we get a lower renormalization factor Z and a higher effective mass $m^* > m$ compared to the perturbative random-phase approximation values.

DOI: 10.1103/PhysRevB.79.041308 PACS number(s): 71.10.Ay, 71.10.Ca, 05.30.Fk, 02.70.Ss

The Fermi-liquid theory of Landau[1] postulates a one-to-one mapping of low-energy excitations of an interacting quantum system with that of an ideal Fermi gas via the distribution function of quasiparticles of momentum k. The resulting energy functional has been successfully applied to describe equilibrium and transport properties of quantum Fermi liquids: the most prominent are the electron gas and liquid ^{3}He.[2,3] However, quantitative microscopic calculations of its basic ingredients, the renormalization factor Z, and the effective mass m^* remain challenging.

In this Rapid Communication, we calculate these parameters for the two-dimensional electron gas (2DEG) using quantum Monte Carlo (QMC) in the region $1 \le r_s \le 10$, where $r_s = (\pi n a_B^2)^{-1/2}$ is the Wigner-Seitz density parameter, n is the density, and $a_B = \hbar^2/(me^2)$ is the Bohr radius. Kwon *et al.*[4] made an attempt to determine the Fermi-liquid parameters of the two-dimensional electron gas using QMC, with results that differ from calculations based on other methods.[5–7] In particular, Kwon *et al.*[4] found an effective mass smaller than the bare mass, e.g., $m^* < m$ at $r_s = 1$. However, QMC calculations suffer from severe finite-size effects since typical system sizes are limited to $N \sim 100$ electrons. Here we show that there is an extremely slow convergence of the effective mass and the renormalization factor to their thermodynamic limit values, with leading-order corrections scaling as $N^{-1/4}$. A correct extrapolation to the infinite-sized system leads to important qualitative and quantitative differences compared to previous calculations[4,7] which had assumed a $(1/N)$ extrapolation. We further use the knowledge of the analytical properties of the ground-state wave function[8] to analytically estimate dominant and subdominant size effects.

Microscopically, the existence and characteristics of the Fermi surface of interacting fermions are directly related to the renormalization factor Z at the Fermi surface.[9] For a normal Fermi liquid, one expects a sharp discontinuity in the momentum distribution $n_{\mathbf{k}}$ at the Fermi surface for each spin,

$$n_{\mathbf{k}} = Z_{\mathbf{k}} \theta(k_F - |\mathbf{k}|) + g_{\mathbf{k}}, \tag{1}$$

where k_F is the Fermi wave vector, $\theta(x)$ is a step function, and $g_{\mathbf{k}}$ is a continuous function of momentum $\mathbf{k}$. One expects a linear excitation spectrum $\varepsilon_{\mathbf{k}} = \hbar^2 k_F (k - k_F)/m^*$ close to the Fermi surface at $|\mathbf{k}| = k_F$, with m^* as the effective mass. The goal is to determine the properties in the $N \to \infty$ limits based on calculations on cells of N particles with discrete values of $n_{\mathbf{k}}^N$ and $Z_{\mathbf{k}}^N$. A microscopic construction of the Landau energy functional is based on considering energy eigenstates which are adiabatically connected to the excited states of the noninteracting Fermi gas.[7] The effective mass is then explicitly given in terms of the energy difference $\varepsilon_{\mathbf{k}} = E_{\mathbf{k}}^{N+1} - (E_0^N + \mu)$ between single-particle excitations of energy $E_{\mathbf{k}}^{N+1}$ and momentum $\mathbf{k}$ and the N-particle ground state of energy E_0^N, where μ is the chemical potential.

QMC methods provide the most accurate calculations of the ground-state energy of the electron gas. However, fermionic QMC calculations suffer from two major drawbacks: the fixed node approximation and finite-size errors. For a normal Fermi liquid, the most precise results are obtained using a generalized Slater-Jastrow form for the trial wave function,[10]

$$\Psi_T \propto D(\mathbf{R}) e^{-U(\mathbf{R})}, \tag{2}$$

where $\mathbf{R}$ indicates a dependence on all particle coordinates. Antisymmetry is assured by a Slater determinant $D(\mathbf{R}) = \det_{ij} e^{i\mathbf{k}_j \cdot \mathbf{q}_i(\mathbf{R})}$ of plane waves inside the Fermi sphere $|\mathbf{k}_j| \le k_F$ using dressed quasiparticle coordinates $\mathbf{q}_i(\mathbf{R})$ to account for many-body backflow effects; whereas the many-body Jastrow potential $U(\mathbf{R})$ is symmetric with respect to particle exchange and accounts for the singularities in the interparticle potential at the coincidence points. Projector Monte Carlo methods can be used to improve the wave function stochastically. Many ground-state properties have been successfully calculated using QMC; however, the situation is less clear concerning excited-state properties.[7]

The Slater determinant of many-body wave function (2) directly connects the ground state of the interacting system

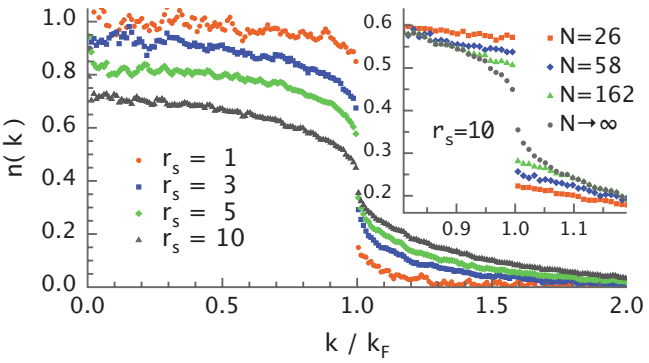

FIG. 1. (Color online) The momentum distribution of $N=162$ unpolarized electrons using grand-canonical twist-average VMC for densities $r_s=1-10$, analytically corrected for size effects around k_F. The inset compares the uncorrected QMC data for different system sizes between $N=26$ and $N=162$ with the size-corrected distribution at $r_s=10$ ("$N\to\infty$").

with the noninteracting one: low-lying excitations are obtained by changing the "occupation numbers" of the plane waves. The energy is therefore a functional of the occupation numbers as postulated within the Landau Fermi theory.[3] Whereas this energy functional certainly exists for any finite system, its existence in the thermodynamic limit is nontrivial; a necessary condition is $\lim_{N\to\infty} Z^N_{k_F}>0$: a central issue of this Rapid Communication.

We have performed variational quantum Monte Carlo (VMC) and diffusion Monte Carlo (DMC) calculations of the 2DEG; the electrons interact with a $1/r$ potential and with a positive background charge. We have used a Slater-Jastrow backflow (SJ-BF) wave functions with an analytical form for both the Jastrow and backflow potentials;[11] all potentials are split in short- and long-range contributions as described in Ref. 12. For $N=58$ electrons, the DMC ground-state energies obtained are $\lesssim 3mRy$ lower than previous calculations using numerically optimized forms.[13] Excited states were formed by adding or subtracting orbitals in the determinant; the backflow and Jastrow forms[11] are independent of the precise occupation of the Slater determinant. Since the trial function had no free parameters, we can study size effects without reoptimizing parameters for different system sizes.

First, we calculated the momentum distribution as explained in Ref. 14. However, for systems in periodic boundary conditions, the momentum distribution is only given at discrete values $\mathbf{k}=2\pi(n\hat{\mathbf{x}}+m\hat{\mathbf{y}})/L$, where n and m are integers and $\hat{\mathbf{x}}$ and $\hat{\mathbf{y}}$ are the unit vectors in the x and y directions, respectively. Using twisted boundary conditions with twist angles $(\theta_x\hat{\mathbf{x}}+\theta_y\hat{\mathbf{y}})2\pi/L$ for the trial wave functions, we can obtain a momentum distribution for all values of $\mathbf{k}$ by varying the twist angle. In the limit of an infinite-sized system, the Slater determinant of our trial wave function approaches a sharp Fermi surface, occupying only wave vectors $|\mathbf{k}|\le k_F$. For finite systems, the sharp behavior of the occupation numbers inside the Slater determinant is best described by working in the grand-canonical ensemble using only orbitals inside the Fermi sphere for a given twist angle.[8,15] As shown in Fig. 1, the renormalization factor quantifying the jump in the momentum distribution at k_F can be precisely read off for any finite system. However, strong size effects around the Fermi surface are still evident.

We can analyze size effects directly using the analytical form of the SJ-BF trial wave function. The momentum distribution is obtained by displacing one particle $\mathbf{r}_j$ a distance $\mathbf{r}$,

$$n^N_{\mathbf{k}}=\left\langle e^{-i\mathbf{k}\cdot\mathbf{r}-\delta U_N}\frac{D(\mathbf{R}:\mathbf{r}_j+\mathbf{r})}{D(\mathbf{R})}\right\rangle, \tag{3}$$

where $\langle\cdots\rangle$ denotes averaging over $|\Psi_T(\mathbf{R})|^2$ and over a uniform distribution for $\mathbf{r}$; the change in the Jastrow potential in terms of its Fourier transform u_q is

$$\delta U_N=\frac{1}{V}\sum_{\mathbf{q}\neq 0} u_q[e^{i\mathbf{q}\cdot\mathbf{r}_j}\rho_{-\mathbf{q}}-1][e^{i\mathbf{q}\cdot\mathbf{r}}-1], \tag{4}$$

where $\rho_{\mathbf{q}}=\Sigma_j e^{i\mathbf{q}\cdot\mathbf{r}_j}$. As described in Ref. 8, the most important finite-size effects can be understood as an integration error by analytical continuation of the finite-size (periodic) wave function to an infinite system where the estimator in Eq. (3) would contain the following change in the Jastrow factor:

$$\delta U_{N\to\infty}\to\int\frac{d^2\mathbf{q}}{(2\pi)^2}u_q[e^{i\mathbf{q}\cdot\mathbf{r}_j}\rho_{-\mathbf{q}}-1][e^{i\mathbf{q}\cdot\mathbf{r}}-1]. \tag{5}$$

The finite-size correction is then dominated by the nonanalyticity of the integrand at $q=0$,

$$\delta U_\infty-\delta U_N\simeq\int_{-\pi/L}^{\pi/L}\frac{d^2\mathbf{q}}{(2\pi)^2}u_q[e^{i\mathbf{q}\cdot\mathbf{r}_j}\rho_{-\mathbf{q}}-1][e^{i\mathbf{q}\cdot\mathbf{r}}-1],$$

and we can calculate the leading-order size corrections $\delta n_{\mathbf{k}}\equiv n^\infty_{\mathbf{k}}-n^N_{\mathbf{k}}$ by expanding $n^\infty_{\mathbf{k}}$ [Eq. (3)] up to the second order in $\delta U_\infty-\delta U_N$. Neglecting mode-coupling terms, we get

$$\begin{aligned}\delta n_{\mathbf{k}}\simeq&\int_{-\pi/L}^{\pi/L}\frac{d^2\mathbf{q}}{(2\pi)^2}\delta(q)[n^N_{\mathbf{k}+\mathbf{q}}-n^N_{\mathbf{k}}]\\&+\int_{-\pi/L}^{\pi/L}\frac{d^2\mathbf{q}}{(2\pi)^2}\int_{-\pi/L}^{\pi/L}\frac{d^2\mathbf{q}'}{(2\pi)^2}u_qu_{q'}[1-S(q)-S(q')]\\&\times[n^N_{\mathbf{k}}+n^N_{\mathbf{k}+\mathbf{q}+\mathbf{q}'}-n^N_{\mathbf{k}+\mathbf{q}}-n^N_{\mathbf{k}+\mathbf{q}'}],\end{aligned} \tag{6}$$

where

$$\delta(q)=\{u_q[1-S(q)]-nu_q^2S(q)\}. \tag{7}$$

Equation (6) expresses size corrections in terms of the long-wavelength limits of the Jastrow potential u_q and of the structure factor $S(q)$. In the limit $q\to 0$, we have

$$\begin{aligned}2nu_q&\simeq -1+[1+(2nv_q/\varepsilon_q)]^{1/2},\\S(q)&\simeq[2nu_q+1/S_0(q)]^{-1},\end{aligned} \tag{8}$$

where $v_q=2\pi e^2/q$, $\varepsilon_q=\hbar^2q^2/2m$, and $S_0(q)$ is the structure factor of the noninteracting Fermi gas.

As the momentum distribution of a Fermi liquid [Eq. (1)] is smooth everywhere away from the Fermi surface, leading-order corrections are restricted to a small region around k_F, where we can write

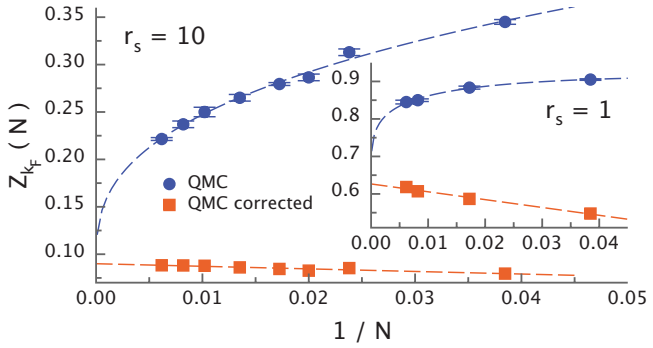

FIG. 2. (Color online) The renormalization factor Z for $r_s=10$ estimated from the finite-size momentum distribution as a function of the inverse number of electrons and the corresponding size-corrected values. Dashed lines illustrate the size corrections of order $N^{-1/4}$ (N^{-1}) for the uncorrected (corrected) data. The inset shows the corresponding values at $r_s=1$.

$$\delta n_{\mathbf{k}} \simeq Z_{k_F}^N \int_{-\pi/L}^{\pi/L} \frac{d^2\mathbf{q}}{(2\pi)^2} \delta(q)[\theta(k_F - |\mathbf{k}+\mathbf{q}|) - \theta(k_F - k)]. \tag{9}$$

In Fig. 1 we show the size-corrected momentum distribution for different densities between $r_s=1$ and $r_s=10$ using Eq. (9). Close to k_F, size effects lead to important qualitative and quantitative changes.

The renormalization factor Z can be read off directly from the jump of the momentum distribution at the Fermi surface, $Z_{k_F}^N = n_{k_F-\epsilon}^N - n_{k_F+\epsilon}^N$, and its size-corrected value may therefore be read off directly from Fig. 1. For a precise evaluation of Z in the thermodynamic limit, we have studied the extrapolation separately. From Eq. (6), one can show that size corrections of Z can be written as

$$Z_{k_F}^\infty \simeq Z_{k_F}^N e^{-\Delta_N}, \quad \Delta_N = \int_{-\pi/L}^{\pi/L} \frac{d^2\mathbf{q}}{(2\pi)^2} \delta(q), \tag{10}$$

which includes the main subleading-order corrections. Using analytical forms (7) and (8), the leading-order corrections are

$$\Delta_N \simeq \left(\frac{\pi r_s^2}{4N}\right)^{-1/4} \quad \text{for} \quad N \to \infty. \tag{11}$$

Asymptotic form (10) with Eq. (11) shows that actual QMC calculations with typically $N \sim 10^2$ electrons suffer from very strong size effects. Obscured by the intrinsic noise of QMC calculations, pure numerical analysis of the data might suggest convergence in the thermodynamic limit to values very different from the exact value.

In Fig. 2 we compare the bare data for $r_s=1$ and $r_s=10$ with their size-corrected values. Whereas the bare data are in reasonable agreement with previous QMC results,[7,14] a numerical extrapolation of the uncorrected data strongly depends on assumptions on the asymptotic scaling form, as size corrections overwhelmingly dominate the calculation of Z. In order to go beyond leading order, we have directly used Eq. (10) together with asymptotic forms (7) and (8) to correct our bare data analytically. As can be seen from the figure, the size-corrected values drastically reduce size effects, as expected. More important, in contrast to the uncorrected data, the extrapolation of the size-corrected values is not sensitive to assumptions on the remaining corrections for densities $r_s \geq 3$. Approaching the high-density region $r_s \lesssim 1$, the thermodynamic limit extrapolation becomes more difficult since the asymptotic expansion is singular in the limit $r_s \to 0$. In Table I we have summarized our results for the renormalization factor.

TABLE I. Energies per particle (in Ry), E_{VMC}, and E_{DMC}, the renormalization factor Z, and the effective mass m^*/m extrapolated to the thermodynamic limit [both within VMC and from perturbative RPA calculations (Ref. 5)]. Values in () are standard errors in the last decimal place.

r_s	1	3	5	10
E_{VMC}	−0.4179(2)	−0.4223(1)	−0.2975(1)	−0.16952(1)
E_{DMC}	−0.4206(2)	−0.4241(1)	−0.2991(1)	−0.17070(1)
Z_{VMC}	0.62(4)	0.34(3)	0.22(2)	0.090(4)
m^*/m_{VMC}	1.26(7)	1.39(8)	1.54(7)	1.72(9)
Z_{RPA}	0.66	0.44	0.34	0.24
m^*/m_{RPA}	1.02	1.12	1.16	1.21

Size corrections of the momentum distribution induce corrections to the total kinetic energy which can be shown to coincide with the two-dimensional analog of Ref. 8. In two dimensions, the leading-order size corrections of the kinetic and potential energies per particle scale as $N^{-5/4}$ in the Fermi-liquid phase. We show VMC and DMC energies of the size-extrapolated values of the energy per particle in Table I.

Since this class of wave functions has $Z>0$, the single-particle excitation spectrum should be dominated by quasiparticle excitations with an effective mass m^*. We have calculated the effective mass by adding an electron with momentum $\mathbf{p}$ with $|\mathbf{p}|>k_F$ to the ground state. The effective mass of an excited state is determined assuming an expansion of the self-energy in powers of $p-k_F$, leading to $2m\varepsilon_p/\hbar^2 = p^2 - k_F^2 + 2k_F(m/m^* - 1)(p-k_F)$ in the vicinity of k_F.

Again, the proper treatment of size effects is essential to extrapolate to the thermodynamic limit. The additional electron at momentum $\mathbf{p}$ will induce size corrections in the momentum distribution which can be estimated as before. The resulting additional finite-size error in the total kinetic energy $\delta T_{\mathbf{p}}^N$ due to the excitation of momentum $\mathbf{p}$ is then given by

$$\delta T_{\mathbf{p}}^N = \frac{\hbar^2\mathbf{p}^2}{2m} Z_{\mathbf{p}}^N [e^{-\Delta_N} - 1]. \tag{12}$$

We see that the size corrections of the effective mass are intrinsically related to those of the renormalization factor Z, leading to a similar asymptotic scaling law $N^{-1/4}$. Potential-energy corrections are independent of $\mathbf{p}$ in leading order and Eq. (12) dominates finite-size corrections for m/m^*. Note that the renormalization factor can also be obtained from analyzing the finite-size error of effective-mass calculations without explicit calculations of the momentum distribution.

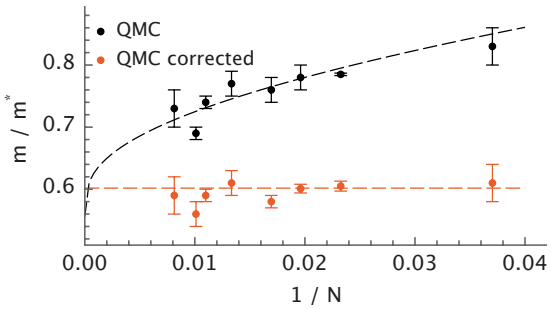

FIG. 3. (Color online) The inverse effective mass m/m^* for $r_s=10$ as a function of N^{-1} together with the corresponding size-corrected values. Dashed lines illustrate the expected size corrections.

From Fig. 3, we see that size effects play a similar important role in determining m^* as they do in determining Z. In particular, for high densities, size effects qualitatively change the conclusion in previous calculations.[4] Whereas, in agreement with Ref. 4 all bare data indicate an effective mass smaller than the bare mass for $N \lesssim 100$, in the thermodynamic limit the effective mass is increased, as predicted by perturbative random-phase approximation (RPA) calculations.[5,6]

Calculations based on many-body perturbation theory going beyond the perturbative RPA approximation have been suggested. However, based on different approximations, these predictions may lead to an enhancement or depression of Z (or the effective mass)[5,6] and it is difficult to estimate reliably the validity of the underlying approximations. Our VMC results for Z are always below the corresponding values of the perturbative RPA calculations, whereas we predict a higher effective mass m^*/m. Our calculations therefore support improved RPA calculations based on many-body local-field theory including charge- and spin-density fluctuations as proposed in Ref. 6.

We have shown that long-range Jastrow potentials lead to strong size effects for the Fermi-liquid parameters. It is interesting to note, however, that modification of the long-range properties can also induce a vanishing renormalization factor Z implying the possibility of describing non-Fermi-liquid behavior within SJ-BF.[16] As our finite-size analysis shows, this is realized, for example, in the case of two-dimensional charges with a logarithmic interaction at long range ($1/q^2$ in reciprocal space).

This research was supported by NSF under Grant No. DMR04-04853, IDRIS Computers, and the ACI "Désordre et Interactions Coulombiennes" and facilitated by the Project de Collaboration CNRS/UIUC. M.H. thanks S. Moroni, C. Pierleoni, R. Chitra, and A. Pasturel for discussions.

[1] L. D. Landau, Sov. Phys. JETP **30**, 1058 (1956).
[2] D. Pines and P. Nozières, *The Theory of Quantum Liquids* (Addison-Wesley, Reading, MA, 1989).
[3] G. Baym and C. Pethick, *Landau Fermi Liquid Theory* (Wiley-VCH, Weinheim, 2004).
[4] Y. Kwon, D. M. Ceperley, and R. M. Martin, Phys. Rev. B **50**, 1684 (1994); **53**, 7376 (1996).
[5] H.-J. Schulze, P. Schuck, and N. Van Giai, Phys. Rev. B **61**, 8026 (2000).
[6] R. Asgari, B. Davoudi, M. Polini, G. F. Giuliani, M. P. Tosi, and G. Vignale, Phys. Rev. B **71**, 045323 (2005).
[7] G. F. Giuliani and G. Vignale, *Quantum Theory of the Electron Liquid* (Cambridge University Press, Cambridge, 2005).
[8] S. Chiesa, D. M. Ceperley, R. M. Martin, and M. Holzmann, Phys. Rev. Lett. **97**, 076404 (2006).
[9] V. M. Galursky and A. B. Migdal, Sov. Phys. JETP **7**, 96 (1958); J. M. Luttinger, Phys. Rev. **119**, 1153 (1960).
[10] M. Holzmann, B. Bernu, and D. M. Ceperley, Phys. Rev. B **74**, 104510 (2006).
[11] M. Holzmann, D. M. Ceperley, C. Pierleoni, and K. Esler, Phys. Rev. E **68**, 046707 (2003).
[12] V. Natoli and D. M. Ceperley, J. Comput. Phys. **117**, 171 (1995); M. Holzmann and B. Bernu, *ibid.* **206**, 111 (2005).
[13] Y. Kwon, D. M. Ceperley, and R. M. Martin, Phys. Rev. B **48**, 12037 (1993).
[14] B. Tanatar and D. M. Ceperley, Phys. Rev. B **39**, 5005 (1989).
[15] C. Lin, F. H. Zong, and D. M. Ceperley, Phys. Rev. E **64**, 016702 (2001).
[16] M. Capello, F. Becca, S. Yunoki, and S. Sorella, Phys. Rev. B **73**, 245116 (2006); F. Krüger and J. Zaanen, *ibid.* **78**, 035104 (2008).